ResearchGate

See discussions, stats, and author profiles for this publication at: https://www.researchgate.net/publication/224274616

3D vessel reconstruction from biplane angiograms using snakes

Conference Paper · October 1998

DOI: 10.1109/CIC.1998.731988 · Source: IEEE Xplore

CITATIONS
23

READS
52

4 authors, including:

Petia Radeva
Autonomous University of Barcelona
414 PUBLICATIONS **3,902** CITATIONS
SEE PROFILE

Ricardo Toledo
Autonomous University of Barcelona
55 PUBLICATIONS **415** CITATIONS
SEE PROFILE

All content following this page was uploaded by Petia Radeva on 16 January 2017.

The user has requested enhancement of the downloaded file. All in-text references underlined in blue are added to the original document and are linked to publications on ResearchGate, letting you access and read them immediately.

3D Vessel Reconstruction from Biplane Angiograms using Snakes

P Radeva, R Toledo, C Von Land, J Villanueva

Computer Vision Centre, Barcelona, Spain

Abstract

In this paper, we propose a physics-based model to segment and reconstruct coronary vessels from biplane angiograms. We use the snake technique to model the vessel, the snake deforms in space to adjust its projections to the image data. In this way, segmentation and 3D reconstruction are unified into the same procedure assuring that only plausible vessel shapes will be detected. The method is general allowing to reconstruct the coronary tree from any angles and distances. The results are encouraging.

1. Introduction

Traditionally, 3D vessel reconstruction techniques follow a bottom-up approach based on image feature extraction and reconstruction by interactively indicating corresponding point projections [1-4] or by exhaustive feature matching [5-8]. However, this approach can not cope with ambiguities in the image interpretation (e.g. in branch or intersection points) nor the lack of precision in determining corresponding image points. In this work, we propose a top-down approach based on a 3D deformable model (B-snake) of the vessels that deforms in an active way, adjusting its projections towards the image features. As a result, the spatial reconstruction and image segmentation are simultaneously obtained by detecting only plausible shapes for the vessels. These shapes are constrained by the physics-based model that implicitly incorporates spatial, continuity and structural constraints.

In 3D vessel reconstruction techniques, spatial position of a vessel point can be recovered by calculating the intersection of projection rays to the corresponding points in biplane images [5]. In practice, due to systematic errors and difficulties in precisely determining corresponding points, a true intersection point does not exist. In these cases, the minimum distance reconstruction method is applied [2]. In this paper, we achieve this by optimizing the B-snake model, so that the distance between projection rays for each 3D point is minimised. In addition, in the B-snake approach all points of the vessels contribute to the 3D reconstruction instead of using a sparse set of points (usually, the bifurcation points). Furthermore, taking into account that the isocenter is not a sharp and stable point, we include its position in the optimization process to simultaneously refine global (related to the isocenter) and local (related to the vessel co-ordinates) parameters.

The 3D reconstruction angiography approach by snakes has been proposed in [9] to recover 3D catheter paths in angiographic images. Here, we extend this approach refining the external force derived from image data, generalizing the method for any angles and number of views and including global (related to the isocenter) parameters into the optimization scheme.

The article is organized as follows: in the next section we give a brief description of the geometry that defines the biplane angiography. In section 3 we briefly explain the snake technique and its application to the 3D reconstruction of the vessels. The paper finishes by discussing the results and presenting some conclusions.

2. Biplane imaging geometry

Standard biplane angiographic devices consist of two X-ray systems that can be rotated independently from each other. Two rotation axes are allowed: a horizontal axis in longitudinal direction with the table and a horizontal axis perpendicular to the table. The left-right movement of a system with respect to the patient defines the rotation angle. The angles by which a movement can be defined towards the head of the patient (cranial direction) or the feet (caudal direction) represent the angulation angles [2]. The projection axes of both systems intersect in the *isocenter*. The distances from the X-ray sources to the image intensifiers are predetermined before the image acquisition process.

3D reconstruction techniques require a global reference system. In our case, the isocenter coincides with the origin of the co-ordinate system (see fig. 1). The x axis is horizontally directed in longitudinal direction of the table, the y axis is horizontal directed towards the left arm of the patient and the z axis is

0276-6547/98 $10.00 © 1998 IEEE

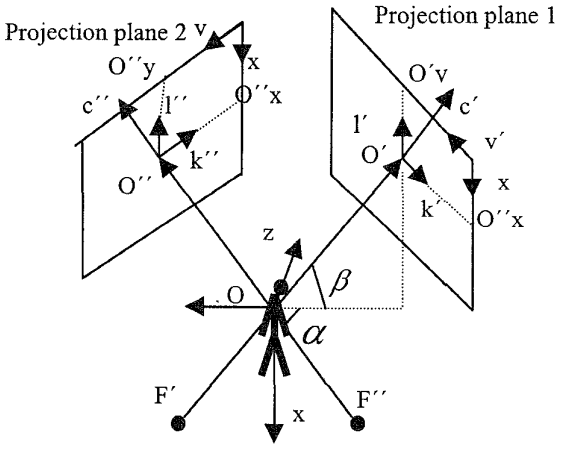

Fig.1 Global reference system *(x,y,z)* with the projection planes and their local co-ordinate systems *(k',l',c')* and *(k'',l'',c'')*. *F'* and *F''* represent the X-ray source positions.

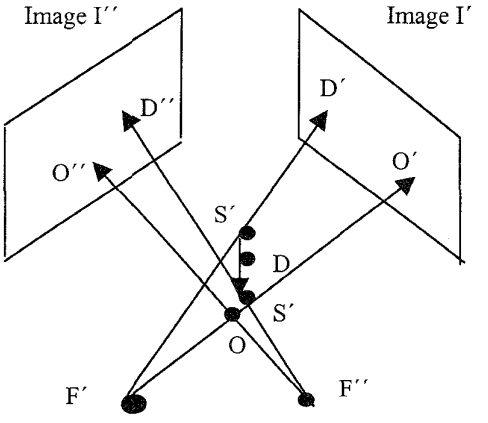

Fig. 2 The minimum distance reconstruction of corresponding points D'and D''.

vertically directed and upwards. The local reference systems are chosen as left-hand oriented, triple orthogonal systems determined as follows [2]:

$$k = \left(0, \cos\alpha, sin\alpha\right)^T$$

$$l = \left(-\cos\beta, sin\alpha\, sin\beta, \cos\alpha\, sin\beta\right)^T$$

$$l = \left(sin\beta, sin\alpha\cos\beta, \cos\alpha\cos\beta\right)^T$$

where alfa and beta give the angulation and rotation angles. The vector *c* indicates the direction of the central beam of the X-ray cone while the vectors *k* and *l* are in the opposite direction of the image axes *x* and *y*.

In order to reconstruct a point in a 3D space from several projections, its image points should be identified. The intersection point of the projection rays from the X-ray sources to the image points defines the 3D point. Given the acquisition parameters (X-ray source position, isocenter position, angulation and rotation angles and calibration factor *m* defined by the ratio of the true size of an object in mm to its projected size in pixels), the exact 3D position can be found.

Let us consider a point D and its projections D' and D'' in two image planes. The intersection point of lines F'D' and F''D'' determines the 3D position of the point D. However, in practice, both lines do not usually intersect (see fig. 2) due to the limited accuracy of the projection geometry and the calibration factor or the presence of geometric image distortion. Then, the spatial location of the point D is computed as the point of minimal distance to both lines by the back-projection expression for the point D as follows [2]:

$$\vec{OD} = \vec{OF'} + \tau\vec{F'D'} + \tfrac{1}{2}\vec{S'S''} \qquad (2)$$

3. 3D reconstruction by snakes

The equation (2) provides an estimation of the 3D position of vessel points given their corresponding image points. However, manually indicating each pair for all vessel points is very tedious and time-consuming. To facilitate the 3D reconstruction, we utilize a snake that is represented as a 3D curve. This elastic curve is deformed in space to adjust its projections to the image data. In this way, the segmentation and the reconstruction processes are integrated and the 3D vessel position is directly obtained. At the same time, only plausible shapes are recovered that agree with the image data and the structural and smoothness constraint of the snake.

3.1. Snake definition

A snake is an elastic curve with associated energy:

$$E = \int E_{\text{int}}(Q(u)) + E_{ext}(Q(u))du$$

where *Q(u)=(X(u),Y(u),Z(u))* is the spatial representation of the snake curve.

From its initial position, the snake is iteratively updated to adjust to the image data while maintaining a smooth shape. The convergence towards the image data is related to the definition of an external energy while the smoothness corresponds to the definition of an internal energy. The solution of the reconstruction process corresponds to a 3D snake that has a minimum energy, i.e. has converged to the closest set of image data that fulfils the smoothness constraint.

The internal snake energy is defined as a sum of the membrane energy that operates like springs attracting successive points of the snake and the thin-plate energy

that prevents the snake from excessive twisting. The external energy of the snake is defined so that it reaches a minimum when it is projected into the vessel projections in the images. To this aim, we apply a ridge detector and then create a potential field P corresponding to each image where the distance to the closest ridge point is assigned to each point of the potential field. In this way, the external energy is minimal when the distance of each projected snake to the closest ridge is negligible.

3.2. Generalized 3D external force

In its original formulation [10], the snake is a planar curve $Q(X(u),Y(u))$ that deforms in the image plane to match the object's contour. The snake energy is minimized by applying the Euler-Lagrange equation that leads to the following equation [10]:

$$Q^{t+1} = (A + \gamma I)^{-1}(\gamma Q^t + F_{ext}), \text{ where} \quad (3)$$

$$F_{ext} = -\nabla P(Q) = -(\frac{dP}{dx}, \frac{dP}{dy})|Q, \gamma \text{ is a damping para -}$$

meter, A is a stiffness matrix[10], P is the potential.

In our case, the snake is a 3D curve, in order to apply (3) its 3D external force should be defined based on the image external forces. We use the relation (1) between a local (k,l,c) and global (x,y,z) co-ordinate systems:

$$x_i = -k_i = \cos\alpha_i y - \sin\alpha_i z$$

$$y_i = -l_i = \cos\beta_i x - \sin\alpha_i \sin\beta_i y - \cos\alpha_i \sin\beta_i z$$

$$\nabla P_i = \frac{dP_i}{dx_i} x_i + \frac{dP_i}{dy_i} y_i = \cos\beta_i \frac{dP_i}{dy_i} x + (\cos\alpha_i \frac{dP_i}{dx_i} -$$

$$\sin\alpha_i \sin\beta_i \frac{dP_i}{dy_i}) y - (\sin\alpha_i \frac{dP_i}{dx_i} + \cos\alpha_i \sin\beta_i \frac{dP_i}{dy_i}) z,$$

where i denotes the image view.

Taking into account the magnification due to the perspective projection, we re-scale the magnitude of the image external force. Considering N projection planes, after term reduction we obtain the following expression for the generalized external force of the 3D snake from the N image potential fields:

$$F_x = \sum_{i=1}^{N} \frac{\lambda_i m_i}{F_i D_i} \cos\beta_i \frac{dP_i}{dy_i} \left[|F_i O| + |OD^t| \right]$$

$$F_y = \sum_{i=1}^{N} \frac{\lambda_i m_i}{F_i D_i} (\cos\alpha_i \frac{dP_i}{dx_i} - \sin\alpha_i \sin\beta_i \frac{dP_i}{dy_i}) \left[|F_i O| + |OD^t| \right]$$

$$F_z = -\sum_{i=1}^{N} \frac{\lambda_i m_i}{F_i D_i} (\sin\alpha_i \frac{dP_i}{dx_i} + \cos\alpha_i \sin\beta_i \frac{dP_i}{dy_i}) \left[|F_i O| + |OD^t| \right]$$

where λ_i is the potential weight of image i and D^t is the estimation of point D at iteration t.

Given an initial snake located near the vessel of interest, at each iteration the snake is projected into the image planes, the external forces from each potential field are estimated, 3D external force is generalized and the iterative equation (3) is applied. An example of vessel reconstruction from anterior and lateral views is shown in fig.3.

3.3. Optimization of the isocenter position

It has been shown [2] that the isocenter is not a sharp and stable point during the image acquisition. Mechanical influences such as gravity and movement tolerances can blur the isocenter to an unsharp cloud. Obviously, the co-ordinates of the isocenter take part in the correct estimation of the projection of the 3D curve model. We consider that the isocenter can suffer small movement as well as small error in its precise estimate. To cope with this problem, we apply an optimization process after each convergence of the snake to update the isocenter co-ordinates. Given N views (images) and M points of the vessel model, an energy function is defined as a sum of the distances of the projections of the obtained model points to the closest image data:

$$H = \sum_{i=1}^{N} \sum_{j=1}^{M} d(D_{ij} G_{ij}) \text{ where } G_{ij} \text{ is the closest}$$

ridge point in potential P_i to the projection of point D_j.

Gradient descent method is applied to the isocenter co-ordinates so that this error function is minimized.
The results showed that the two-step procedure consisting of updating snake parameters and isocenter co-ordinates reduces the error function H assuring better convergence properties and more precise reconstruction during the optimization process (see fig.4).

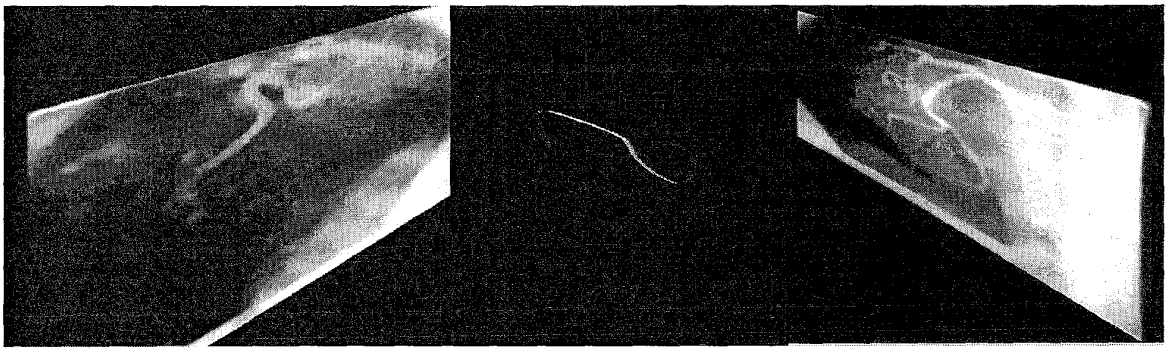

Fig3. Vessel reconstruction by spatial snakes

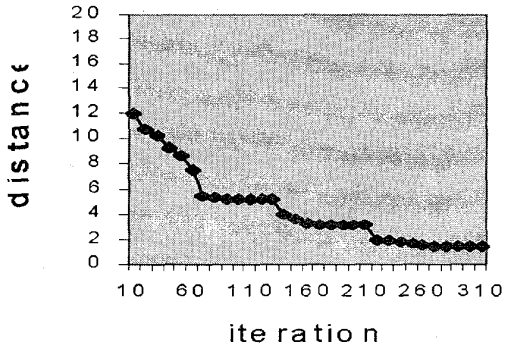

Fig.4 Snake convergence in the two-phase optimization procedure. Isocenter co-ordinates have been updated at iteration 130, 210 and 270.

4. Conclusions

In this paper, we apply a snake model to segment and reconstruct the coronary vessels in a semiautomatic way. The advantages of this approach are that no exact user-provided point correspondence is necessary. The snake evolves in the space to adjust to the image data; as a result the model provides such a correspondence between the image points. The results showed that the technique is optimal from point of view of the minimal reconstruction error defined as the distance between the projection rays. Furthermore, the reconstruction is improved when isocenter co-ordinates are iteratively updated. The results obtained are encouraging and our future research plans include to fuse spatial information from biplane angiograms with structural information provided by intra-vascular ultrasound images.

Acknowledgements

This work was partly funded by research grants from *CICYT* with numbers TIC98-1100 and TAP96-0629-C04-03.

References

[1] Büchi M, Hess OM, Kirkeeide RL, Suter T, Muser M, Osenberg HP, Niederer P, Anliker M, Lance Gould K, Krayenbühl H. Validation of a New Automatic System for Biplane Quantitative Coronary Arteriography. International Journal of Cardiac Imaging 1990; 5:93-103.

[2] Dumay ACM, Reiber JHC, Gerbrands JJ. Determination of Optimal Angiographic Viewing Angles: Basic Principles and Evaluation Study. Med. Imaging 1994; 13(1):13-23.

[3] Wahle A, Oswald H, Schulze GA, Beier J, Fleck E. 3D Reconstruction, Modelling and Viewing of Coronary Vessels. In: Computer Assisted Radiology, 1991:669-76.

[4] Wahle A, Oswald H, Fleck E. 3D Heart-Vessel Reconstruction from Biplane Angiograms. IEEE Computer Graphics and Applications 1996; January:6573.

[5] Coatrieux JL, Garreau M, Collorec R, Roux C. Computer Vision Approaches for the Three-Dimensional Reconstruction of Coronary Arteries: Review and Prospects. Critical Reviews in Bio. Eng. 1994; 22(1):1-38.

[6] Sarwal A, Dhawan A, Chitre Y. 3-D Reconstruction of Coronary Arteries using Estimation Techniques. In: SPIE 1995; 2434:361-9.

[7] Smets C, van de Werf F, Suetens P, Oosterlinck A. An Expert System for teh Labeling and 3D Reconstruction of the Coronary Arteries from Two Projections. International Journal of Cardiac Imaging 1990; 5:145-54.

[8] Yanagihara Y, Hashimoto T, Sugahara T, Sugimoto N. A New Method for Automatic Identification of Coronary Arteries in Standard Biplane Angiograms. International Journal of Cardiac Imaging 1994, 10:253-61.

[9] Molina C, Prause GP, Radeva P, Sonka M. Catheter Path Reconstruction from Biplane Angiography using 3D Snakes. In: SPIE – Medical Imaging, San Diego, 1998.

[10] Kass M,Witkin A, Terzopolous D. Snakes: Active Contour Models. In: ICCV 1987:259-268.

Address for correspondence.

Petia Radeva
Centre de Visió per Computador, UAB
08193 Bellaterra (Barcelona), Spain
Tel 34-93 581 18 62, E-mail: petia@cvc.uab.es

View publication stats